



ELSEVIER

Available online at www.sciencedirect.com

ScienceDirect

journal homepage: www.elsevier.com/locate/he

Aqueous phase reforming of polyols from glucose degradation by reaction over Pt/alumina catalysts modified by Ni or Co

Liza A. Dosso, Carlos R. Vera, Javier M. Grau*

Instituto de Investigaciones en Catálisis y Petroquímica “Ing. José Miguel Parera”- INCAPE (FIQ, UNL-CONICET), CCT CONICET SANTA FE “Dr. Alberto Cassano”, Colec. Ruta Nac. N° 168 KM 0, Paraje El Pozo, S3000AOJ, Santa Fe, Argentina

ARTICLE INFO

Article history:

Received 13 March 2017
Received in revised form
6 June 2017
Accepted 11 June 2017
Available online xxx

Keywords:

Aqueous phase reforming
Polyols
Nickel
Cobalt
Platinum
Urea matrix combustion method

ABSTRACT

A comparison of Pt-M/Al₂O₃ catalysts (M = Ni, Co, none) for the aqueous phase reforming (APR) of different polyols that can be obtained from glucose degradation was made. A standard monometallic Pt/Al₂O₃ catalyst was prepared by incipient wetness impregnation (IWI) of platinum on an alumina support. The bimetallic catalysts had Ni or Co promoters incorporated by the urea matrix combustion method (UCM) and Pt by IWI technique (PtNi and PtCo catalysts).

The catalysts were characterized by ICP/MS analysis, CO/chemisorption, TPR, XPS, SEM-EPMA and XRD. The catalytic activity was assessed with the tests of APR of an aqueous solution of 10 %wt of ethylene glycol (EG), glycerol (Gly) or sorbitol (Sorb), in a tubular fixed bed reactor at 498 K, 2.2 MPa, WHSV = 2.3–2.5 h⁻¹, 3 cm³min⁻¹ He carrier. Monitored variables were: conversion to carbon product in the gas phase, hydrogen and methane yield, selectivities, TOF and coke content on the spent catalysts.

PtNi and PtCo catalysts had better hydrogen yield and stability during the experiments than the un-promoted Pt catalyst, (H₂ yield = 24.4, 21.2 and 15% for PtNi, 17.9 and 15.1 for PtCo and 13.7, 10.8 and 7.5% for Pt after 8 h on stream in APR of EG, Gly or Sorb solution, respectively). Especially PtNi showed excellent yield and selectivity to hydrogen and a good stability, steadily generating hydrogen for long times. Co addition mainly helped in keeping low levels of coke and a low selectivity to methane.

© 2017 Hydrogen Energy Publications LLC. Published by Elsevier Ltd. All rights reserved.

Introduction

It has been implicated that the burning of fossil fuels has a major impact on increasing concentrations of CO₂ in the atmosphere. Energy derived from biomass releases carbon with a carbon-energy ratio similar to that of coal. However,

biomass has already absorbed an equal amount of carbon from the atmosphere before its emission, so that the net carbon emissions of biomass fuels are zero during their life cycle [1]. The production of hydrogen from bio-renewable sources could result promising to minimize environmental problems associated with the combustion of fossil fuels [2].

* Corresponding author.

E-mail address: jgrau@fiq.unl.edu.ar (J.M. Grau).

<http://dx.doi.org/10.1016/j.ijhydene.2017.06.100>

0360-3199/© 2017 Hydrogen Energy Publications LLC. Published by Elsevier Ltd. All rights reserved.

Three main types of processes exist for production of hydrogen and fuels from biomass: gasification to produce syngas, thermo-chemical liquefaction and/or pyrolysis for bio-oils production [3], and acid [4] or enzymatic hydrolysis of lignocellulose [5] for production of sugars that are then refined to produce hydrogen, alkanes, alcohols or aromatic hydrocarbons [6].

Gasification of biomass produces renewable hydrogen, is an efficient clean way for large-scale hydrogen production, and has less dependence on fossil energy sources. Steam reforming of natural gas and gasification of biomass could become the dominant technologies by the end of the 21st century [7].

Catalytic conversion of biomass-derived polyols has recently attracted attention [7]. The conversion of polyols into H_2 can be performed either in gas phase (gas phase reforming, GPR) [8] or liquid phase.

Hydrolysis of biomass can generate different starting compounds for hydrogen production, as shown in Fig. 1 for the case of glucose. These final product alcohols can be transformed into hydrogen over an appropriate catalyst.

Due to the good water solubility of the involved reactants the liquid phase reforming is usually carried out in an aqueous phase (aqueous phase reforming, APR) [9]. Due to the high thermal sensitivity of the reactants, APR is performed at lower temperatures than gas phase reforming [10–12], which is a great advantage.

Advantages of APR cannot be over emphasized: i) the process eliminates the need to vaporize both water and the oxygenated hydrocarbon, which reduces the energy requirements for producing hydrogen; ii) The oxygenated compounds of interest are nonflammable and non-toxic, allowing them to be stored and handled safely; iii) liquid phase reforming shows higher H_2/CO selectivity ratios due to the more favorable conditions for the water-gas-shift thermodynamics, iv) Pressures used during the process (typically 1.5–5.0 MPa) are those where the hydrogen-rich effluent can be effectively purified using pressure-swing adsorption or membrane technologies, and the carbon dioxide can also be effectively separated for either sequestration or use as a chemical; v) APR occurs at low temperatures that minimize undesirable decomposition reactions; vi) production of H_2 from carbohydrates may be accomplished in a single-step, low-temperature process, in contrast to the multi-reactor steam reforming system required for producing hydrogen from hydrocarbons [12].

Catalysts for APR are metallic (normally noble metals of the transition metals group) and can have high loadings of the active metal. Dumesic et al. [12] found that the rate of ethylene glycol reforming decreases in the following order: Pt, Ni > Ru > Rh, Pd > Ir.

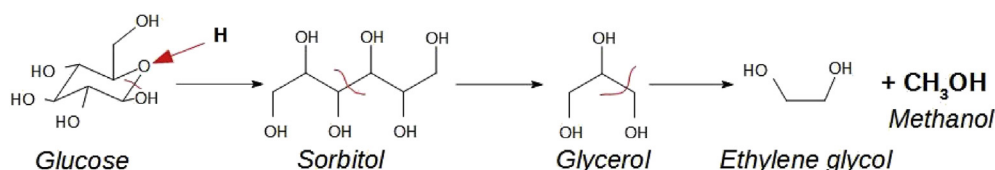


Fig. 1 – Polyols products of Glucose degradation.

APR involves a complex network of elementary reaction steps. In this sense Dumesic et al. [12] have suggested that active catalysts for APR reactions should possess high catalytic activity for the water-gas shift (WGS) reaction and sufficiently high catalytic activity for cleavage of C–C bonds. On this basis, Pt-based catalysts have been identified as promising. Due to their low cost and good catalytic activity, Ni-based catalysts are also attractive despite their undesired activity for producing alkanes. Dumesic et al. [13] have suggested in other reports that alloying Pt with Ni, Co or Fe improves the activity for H_2 production by lowering the *d*-band center, which causes a decrease in the heats of CO and hydrogen adsorption, thereby increasing the fraction of the surface available for the reaction of ethylene glycol.

An analysis of the state-of-the-art catalysts (e.g. Pt/ Al_2O_3) and process conditions shows that catalysis with high noble metal content (e.g. > 3%) [14–17] and highly diluted feedstocks (e.g. 1%) are commonly used [18,19]. In this sense it could be advantageous to use combinations of metals that yield similar activity levels but contain a lower amount of expensive noble metals. Reacting feedstocks of higher concentration could also lead to higher reaction rates and lower requirements for reactor vessel size.

In order to study these aspects the effect of Ni and Co addition on the catalytic activity and selectivity of alumina supported Pt catalysts of low noble metal content is studied in this work. The focus will be put on increasing the hydrogen yield and the stability of the catalyst. The catalysts will be tested in the APR of different polyols coming from glucose degradation: ethylene glycol, glycerol and sorbitol. Feedstocks of low dilution (10 %wt) were used.

Experimental

Catalysts preparation

Three metal supported catalysts were prepared by using a commercial gamma alumina support (Sasol Alumina Spheres 2.5/210). A monometallic Pt/ Al_2O_3 catalyst, with 1% wt Pt was prepared with tetra amine platinum nitrate ($Pt(NH_4)_4(NO_3)_2$, Sigma-Aldrich) aqueous solution by the incipient wetness impregnation technique (IWI), followed by drying, 12 h in a stove at 373 K and finally calcining in an air stream, 3 h at 723 K. This catalyst was named Pt-IWI.

For the modified bimetallic catalysts a combination of two methods was used. Either Ni or Co were added to the alumina support by means of the urea matrix combustion method (UCM) or solution combustion method [20–22] while Pt was added by incipient wetness impregnation (IWI). The necessary amounts of cobalt nitrate or nickel nitrate (in order to obtain

3% wt of metal in the catalyst) and the amount of urea necessary to have a molar ratio of urea/metal equal to 10 were first dissolved in distilled water. Then gamma alumina, sieved to 35–80 mesh was dipped in the solution. The system was stirred gently at 323 K until a slurry was obtained. Then the sample was calcined at 773 K in a muffle furnace for 10 min. The Pt metal (1 %wt) was then added to the support by IWI of a solution of hexachloroplatinic acid (H_2PtCl_6). The catalysts were named as PtNi-Mix and PtCo-Mix.

The use of a mixed technique in the preparation of the bimetallic catalysts was in order to achieve in a first step the greater dispersion and effective anchoring of the promoter, which is also the metal of highest concentration. At a later stage Pt, which is the metal of lowest concentration, can be impregnated without interference or possibility of being covered by the promoter.

The use of a chlorine salt of Pt in the second metal loading step by IWI had the objective of slightly modifying the acidity of the support. This effect was achieved and verified by EDAX microanalysis (Table 2) and by Py-TPD (not show in this paper). This was made on the assumption that an acid environment would favor the dispersion of the metal precursor [23].

Catalysts characterization

Characterization tests were performed to the catalysts calcined and reduced (except those for TPR analyses that were only calcined) in order to test the catalyst structure at the same conditions of the reaction. To minimize the re-oxidation of the metal catalysts after the reduction step, they were cooled down to room temperature in H_2 flow and stored in a closed vessel under inert atmosphere until their characterization.

The chemical analysis of the catalysts was made by inductively coupled plasma (ICP) analysis of the samples after digesting them in an acid solution. The content of the supported metals (Pt, Ni, Co) in the catalysts was determined by mass spectroscopy with inductively coupled plasma (MS/ICP). The equipment used was an ARL 3410 with argon as gas for the plasma. To a properly weighed solid sample, about 20 cm^3 of an aqueous solution of H_2SO_4 (50% vol) were added, and heated to 523 K under reflux on a hot plate until complete dissolution of the solid sample. Once cold they were diluted. Then an aliquot was placed in the nebulizer of the ICP and the concentration of the metal cations was determined from the mass spectrum of the ion source, as measured by means of a quadrupole mass spectrometer.

An assessment of the amount of accessible metal sites on the catalysts was made using CO as a test molecule. CO selectively chemisorbs on the surface metal atoms. The measurement was performed using 0.05 g of catalyst reduced in a hydrogen stream at 773 K. Calibrated pulses of a mixture of diluted CO of known composition (1.46% CO in N_2 , mol basis) were sent to the reactor cell until the surface became saturated. The amount of CO adsorbed was obtained by registering the amount of CO passing through the cell. This was done by converting the CO to methane over a Ni/Kieselguhr catalyst in the presence of H_2 and by measuring the methane in a flame ionization detector connected on line.

The morphology of the catalysts was inspected by scanning electron microscopy (SEM). The SEM equipment also had an EDAX microanalysis probe that was used for a rapid chemical analysis of the elements with atomic number Z greater than 11 (Na) and mass concentrations above 0.5%. The particles on the catalyst surface were identified and the surface composition analyzed. The catalysts and a sample of the alumina support were analyzed by SEM to determine if a variation between the support and the supported metal catalysts could be microscopically observed. Sample preparation was relatively easy, SEM only requiring the samples to be conductive. For this reason the sample was coated with a thin layer of as gold.

XPS measurements were used to determine the chemical state of the active metal components on the surface of the synthesized catalysts. In Pt/ Al_2O_3 catalysts the Al2p support signal overlaps with the Pt4f signal, usually used for the analysis of Pt. This complicates the direct analysis of Pt from its strongest signal. To solve this problem we used a sign of lower intensity, Pt4d, which does not overlap with the spectral lines of the other components.

X-ray diffraction tests were performed in an XD-D1 Shimadzu diffractometer. A sample of about 0.3 g was dried in an oven and then ground to a powder. Then it was placed on a sample holder and irradiated with $\text{CuK}\alpha$ monochromatic radiation of a wavelength of about 1.54 Å, filtered with Ni, operated at 40 kV and 40 mA, at a scan rate of 2°min^{-1} and scanning the $20\text{--}80^\circ 2\theta$ range.

Temperature programmed reduction (TPR) allows the study of the reducibility of the surface species on the solid support and the degree of interaction between them, especially metal-metal, metal-promoter and metal-support interactions. Reducibility was measured by H_2 consumption as the sample was subjected to a heating schedule. An Ohkura TP 2002s equipment with a thermal conductivity detector (TCD) was used for these experiments. A known mass of catalyst was first treated in flowing air at 723 K for 1 h and then cooled down to room temperature. Then the sample was flushed with flowing Ar for 15 min and the reducing mixture (5% H_2 in Ar) was passed over the sample at room temperature. Once the system was stabilized the temperature was raised linearly from room temperature to 973 K at a heating rate of 10K min^{-1} .

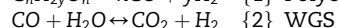
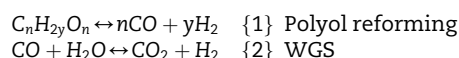
Catalytic activity tests

The reaction of cyclohexane dehydrogenation (CHD) is a known test of the metal function of the catalyst. The reaction is not sensitive to the catalysts structure [24] and the catalytic activity registered is strictly proportional to the concentration of exposed metal atoms, with disregard of the crystal size. The experiments were performed in a glass reactor. The catalyst mass used was 0.1 g, the reaction conditions were: 573 K, 1.01 MPa, hydrogen flow rate $80 \text{cm}^3\text{min}^{-1}$, cyclohexane flow $1.61 \text{cm}^3\text{min}^{-1}$. Cyclohexane was supplied by Merck (99.9%). Previously the catalyst was reduced at 773 K for 1 h with hydrogen. Samples were taken every 5 min and the reaction was terminated after 1 h. The products were analyzed on-line in a gas chromatograph having a 100 m long copper capillary column with 0.5 mm diameter and coated with squalene as stationary phase.

The aqueous phase reforming (APR) of alcohols was carried out in a tubular fixed bed reactor of 9.5 mm internal diameter, made of AISI 316L steel and of 1.5 mm thickness. The reactor was heated by an electric oven. The equipment setup was similar to that used by Dumesic et al. [25]. Reaction conditions were chosen as those yielding higher selectivity to H₂ according to previous reports [25–27]. The chosen pressure had to be slightly higher than the vapor pressure of the feed in order to keep it in the liquid state. Experiments were performed with 0.5 g of catalyst previously reduced in situ in a H₂ stream at 773 K for 1 h, and then flushed with He. The reaction temperature and pressure were controlled to a narrow margin (± 5 °C, ± 0.1 bar). Helium was used to initially purge the system and achieve the desired system pressure. Then the liquid feed was injected to the reactor. The system pressure was regulated with a back-pressure regulator. Reagents were injected with a Cole-Parmer HPLC pump. At the reactor exit the products were cooled down in a condenser and separated in a gas-liquid separator drum. The gases were analyzed with a Shimadzu 8A chromatograph connected on line and equipped with a TCD and a Restek ShinCarbon ST Micropacked column. The feed was an aqueous solution of 10% alcohol injected at a rate of 0.02 cm³min⁻¹. The reaction was performed at 498 K, 2.2 MPa and a gas flow of 3 cm³min⁻¹. The alcohols used were ethylene glycol (EG), glycerol (Gly) and sorbitol (Sorb). Depending on the used feedstock WHSV values were 2.3 h⁻¹ (EG), 2.5 h⁻¹ (Gly) and 2.3 h⁻¹ (Sorb). Long experiments of 600 min were performed in order to check the stability of the catalysts. In all these experiments values of hydrogen yield, carbohydrate conversion and selectivity values to hydrogen, methane, CO and CO₂ were determined, according to [12]:

$$H_2 \text{ yield} = \frac{F_{H_2}^{exp}}{F_{H_2}^{max}} \times 100$$

This is not the common definition of yield, but is that used by Dumesic and coworkers. It has been adopted here for the sake of comparison. $F_{H_2}^{exp}$ is the molar hydrogen flowrate measured at the reactor outlet. As no hydrogen is fed to the reactor this is equal to the produced hydrogen. $F_{H_2}^{max}$ is the hypothetical hydrogen flowrate produced if all the polyol feedstock were reformed according to:



For calculating $F_{H_2}^{max}$ {1} and {2} are considered to be irreversible.

$$C \text{ conversion to gas} = \frac{C \text{ in the gas products}}{C \text{ fed to the reactor}} \times 100$$

$$H_2 \text{ Selectivity} = \frac{H_2 \text{ in the gas products}}{C \text{ in the gas products}} \times \frac{1}{R} \times 100$$

where R is the H₂/CO₂ ratio for the reforming global reaction. $C_nH_{2y}O_n + nH_2O \leftrightarrow nCO_2 + (y+n)H_2$ {1} + n {2} global reaction

$$R = \frac{(y+n)}{n}$$

in this case R = 5/2 for EG, 7/3 for Gly and 13/6 for Sorb.

$$CH_4 \text{ Selectivity} = \frac{CH_4 \text{ in the gas products}}{C \text{ fed to the reactor}} \times 100$$

$$CO \text{ Selectivity} = \frac{CO \text{ in the gas products}}{C \text{ fed to the reactor}} \times 100$$

$$CO_2 \text{ Selectivity} = \frac{CO_2 \text{ in the gas products}}{C \text{ fed to the reactor}} \times 100$$

Other parameter that was compared for the studied catalyst was the Turn-over-frequency for hydrogen production (TOF^{H₂}), in mol of H₂ per unit time and surface metal site. In the evaluation of the rates of H₂ formation expressed as TOF^{H₂}, the number of surface metal sites has been assumed for simplicity to be equal to the amount of irreversibly chemisorbed CO at 300 K, as it is considered by Davda et al. [25].

$$TOF^{H_2} = \frac{\text{mol } H_2 \text{ in the gas product}}{\text{mol CO chemisorbed on surface metal atoms} \times \text{min}}$$

Deactivation study

The deactivation by coking was assessed by temperature programmed oxidation (TPO) of the coke deposits of the used catalysts. An amount of 0.05 g of deactivated catalyst was loaded to a quartz reactor and then combusted with an oxidizing gas mixture (2% O₂ in N₂, molar basis, 30 cm³ min⁻¹ flow rate). The reactor was heated at a rate of 10 K min⁻¹ from room temperature up to 973 K. In the presence of oxygen the deposits are combusted to CO and CO₂. These are transformed into CH₄ over a Ni/kieselguhr catalyst in a methanation reactor and then sent to a flame ionization detector. The TPO trace is thus obtained by registering the FID voltage as a function of the cell temperature. The area under the trace is proportional to the amount of deposited coke.

Results and discussion

Characterization results

Table 1 shows some properties of the metal function of the catalysts: the chemical composition, CO chemisorption capability, hydrogen consumption during the TPR experiment and activity in dehydrogenation of cyclohexane (CHD). Pt-IWI catalyst had the highest capacity for CO chemisorption and dehydrogenating activity. PtNi-Mix had the lowest CO chemisorption capacity, 44.2% that of monometallic Pt, while PtCo-

Table 1 – Results of chemical composition, CO chemisorption, H₂ consumption in TPR experiments and catalytic activity in dehydrogenation of cyclohexane.

Catalyst	Pt%	Ni%	Co%	μmol CO/g cat.	μmol H ₂ /g cat	CH conv., %
Pt-IWI	0.98	–	–	48.7	391.3	93.4
PtNi-Mix	1.05	2.94	–	21.5	682.1	86.2
PtCo-Mix	1.03	–	2.89	33.4	451.6	85.9

Mix had 68.6% the capacity of single Pt. Both promoters, Ni and Co, slightly reduce the dehydrogenating activity of platinum. The decreased capacity for CO chemisorption of Ni promoted Pt catalysts has already been observed by some authors. Ko et al. [28] measured CO chemisorption on mono- and bimetallic catalysts of Ni and Pt supported on γ -Al₂O₃ to study the preferential oxidation (PROX) of CO in a hydrogen rich stream. They found that the addition of Ni decreased the amount of surface active sites for CO chemisorption. However, Pt–Ni was noticeably superior to Pt catalysts for PROX. The authors explained this fact by attributing a higher activity per unit site to the Pt–Ni catalyst. In our case, the decrease in CO chemisorption and dehydrogenation activity should not be related to a decrease in the number of active sites, because the Pt precursor is impregnated after the incorporation of the promoter to the support. A decrease in the capacity of adsorption of Pt because of partial alloying with Ni is more likely. Pt and Ni are completely miscible in solid-solid alloys, in contrast to other metals that are immiscible (e.g. Ru–Cu) or have miscibility gaps (e.g. Pt–Au, Pt–Rh) [29]. In this sense Pt and Ni atoms in close proximity can become readily alloyed during sintering treatments in reducing atmosphere. Alloying of Pt with Ni is known to alter its electronic properties and hence its catalytic ones. The *d*-band center is shifted by (–2.03 eV) resulting in a lesser binding of adsorbates as compared to pure Pt [30].

Micrographs of the PtCo-Mix catalyst particles can be seen in Fig. 2. A and B are different areas studied on the sample. Table 2 shows the EDAX results of the surface chemical composition. We can see that the Pt:Co atomic ratio is close to 1:7, indicating a high concentration of Co on the particle surface. This is a higher Pt:Co ratio than the global one of the fresh catalyst. This result points to a surface enrichment of Pt. The microanalysis also detects surface chlorine, supposedly associated to the remaining ligands of the chloroplatinic acid precursor.

Micrographs of the PtNi-Mix catalyst particles can be seen in Fig. 3. The first micrograph is an overview of the catalyst while the second is a zoomed-in view. In both cases the concentration of the elements was calculated by EDAX (Table 3).

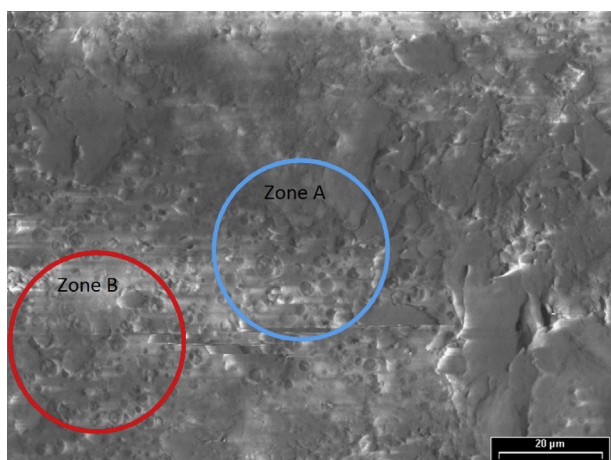


Fig. 2 – Micrograph of the PtCo-Mix catalyst. The circles indicate two zones (A and B) chosen for EDAX analysis.

Table 2 – Results of EDAX micro analysis. PtCo-Mix catalyst sample.

Element	Zone A		Zone B	
	Wt %	At %	Wt %	At %
Al	86.96	93.15	84.87	92.40
Cl	4.39	3.58	3.80	3.15
Co	5.83	2.86	7.89	3.93
Pt	2.82	0.42	3.45	0.52

The analysis of the set of particles reveals that the Pt:Ni atomic ratio is 1:5, i.e. five Ni atoms per atom of Pt. The analysis of the surface of the particle shows a Pt:Ni ratio close to 1:2. In both cases, Cl surface is present in a ratio close to 3%.

Ni is in other cases in a higher proportion of about 1:6. Comparing with the previous results it can be seen that the particles have a different Pt:Ni atomic ratio depending on the spot tested. In some areas the catalysts have a greater concentration of Pt but the average ratio is 1 Pt atom per 5 or 6 atoms of Ni. This is closer to the Pt:Ni, Pt:Co molar ratios used in the preparation of the catalysts, which were almost 1:10.

The surface concentration of chlorine was almost constant on the catalyst particles. The Pt:M ratio always indicated a higher concentration of the second metal; i.e. Co and Ni have a lower mass surface concentration than Pt. Chlorine remains on the surface in those catalysts impregnated with chloroplatinic acid.

Fig. 4 shows the XPS results in the spectral region of the Pt4d of all three catalysts, calcined, reduced and degassed in ultrahigh vacuum for 3 h at 473 K. Deconvolution of the spectrum into its individual components indicates the presence of different states of Pt in the catalyst surface: the reduced state (metallic Pt⁰) with binding energy of Pt 4d_{5/2} = 314 eV, and the oxidized states with binding energy Pt 4d_{5/2} = 318 eV for Pt⁴⁺ and binding energy Pt 4d_{5/2} = 315 eV for Pt²⁺ [31–33]. It is known that redox properties of noble metals such as Pt are fixed by its interaction with the support or with other metal dispersed on surface [34–36]. This metal-support or metal-metal interaction makes it possible for Pt to exist on the surface in different oxidation states. Some authors [33] have associated the states of Pt with the corresponding binding energies (E_b) of Pt⁰ (E_b Pt 4d_{5/2} = 314.2 ± 0.3 eV); Pt⁺² (E_b Pt 4d_{5/2} = 315.3 eV ± 0.3 and Pt⁺⁴ (E_b Pt 4d_{5/2} = 317.0 ± 0.3 eV). According to these data and analyzing the spectrum of our sample we could establish that Pt is mostly in the state of Pt⁺² (315 eV), but there is also Pt⁺⁴ (317 eV) and Pt⁰ (314 eV). The analysis of the Pt 4f signals was not possible because there was an overlap with the Al 2d signals.

In the zone of the spectrum corresponding to Pt4d for the PtNi-Mix catalyst (Fig. 4b), a deconvolution into three peaks, Pt⁺², Pt⁺⁴ and Pt⁰, was possible. This peak had a shift from 314 eV to 316 eV, and was attributed to an increase in the concentration of Pt⁺⁴. This shift could indicate that Pt donated electrons for the formation of Ni⁰. For the PtCo-Mix catalyst (Fig. 4c) platinum showed mainly oxidized species and a small portion of metallic Pt⁰.

The catalyst PtNi-Mix was analyzed in the region Ni2p and especially in the range 850–870 eV (Fig. 5). In this spectrum the deconvolution can be achieved thanks to a double peak at

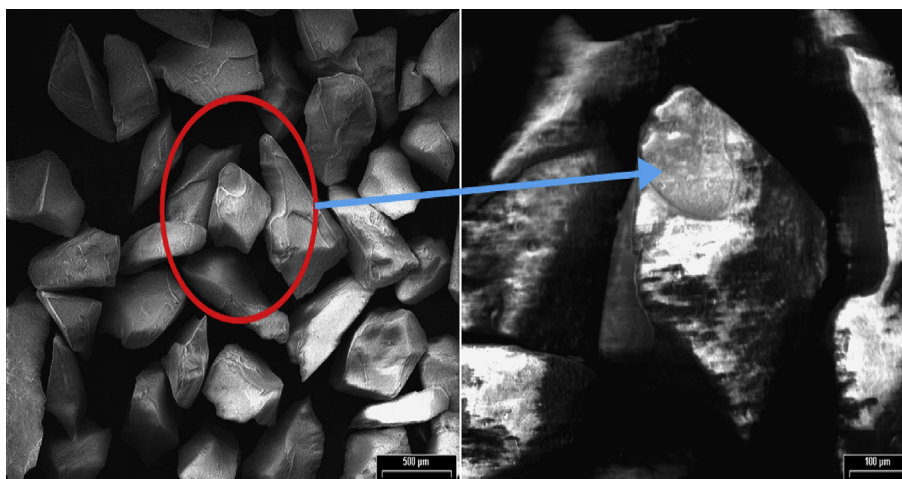


Fig. 3 – Micrograph of the PtNi-Mix catalyst. Zones used in the EDAX analysis: a group of particles (left) and a single particle (right).

Table 3 – Results of EDAX micro analysis. PtNi-Mix catalyst sample.

Element	Group of particles				Single particle surface			
	With Cl		Without Cl		With Cl		Without Cl	
	Wt %	At %	Wt %	At %	Wt %	At %	Wt %	At %
Al	81.65	91.58	84.30	94.20	84.07	93.47	86.91	96.29
Pt	5.96	0.92	6.31	0.98	7.81	1.20	8.32	1.28
Ni	9.10	4.69	9.39	4.82	4.61	2.35	4.77	2.43
Cl	3.29	2.81	0	0	3.52	2.98	0	0

856 eV belonging to NiO. In other reports on Pt-Ni catalysts supported on alumina [37] an interaction between Pt and Ni after reduction was detected. This was evidenced by a shift of the highest peak of nickel to values of binding energy below 855 eV. In this study such an interaction was not observed (Fig. 7). According to [38] the shift of the highest peak of nickel at values of binding energy to 856 eV indicates a strong Ni-support interaction. The Al2S peak also shows a shift to

119.3 eV and O1s at 531.2 eV, in accord with the presence of NiAl₂O₃.

Additionally the Co spectral region of the PtCo-Mix catalyst showed satellite and main peaks that were attributed to Co⁺² signals due to CoO (Fig. 6).

Summarizing the XPS results for all catalysts, it can be seen that Pt²⁺ is the Pt species with the highest surface concentration, while Co²⁺ is the dominant species in the case of the

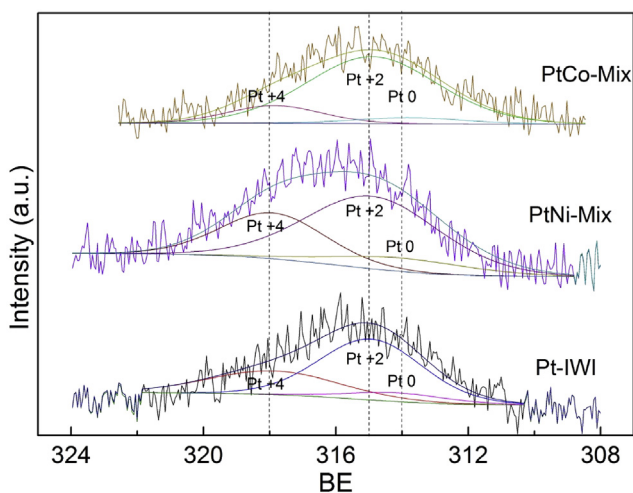


Fig. 4 – XPS spectrum, Pt4d_{5/2} zone, of the reduced studied catalysts.

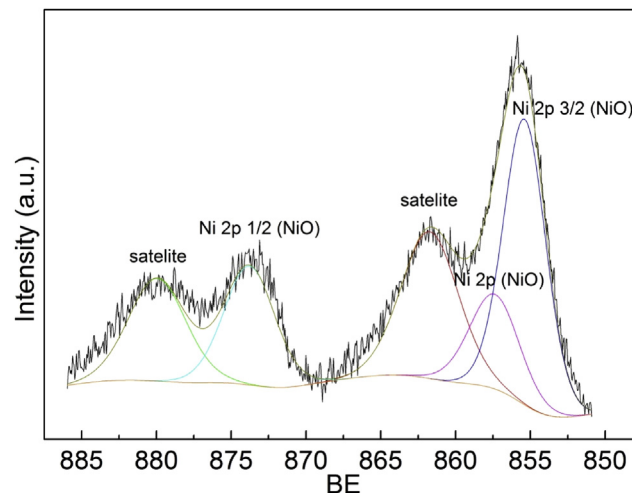


Fig. 5 – XPS spectrum, Ni2p zone of the reduced PtNi-Mix catalyst.

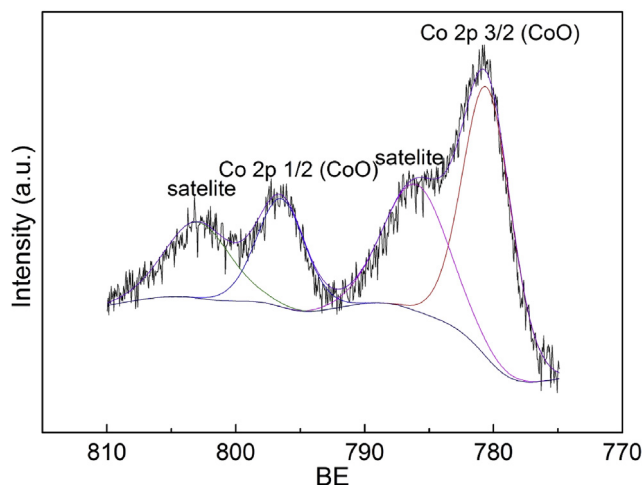


Fig. 6 – XPS spectrum, Co2p zone of the reduced PtCo-Mix catalyst.

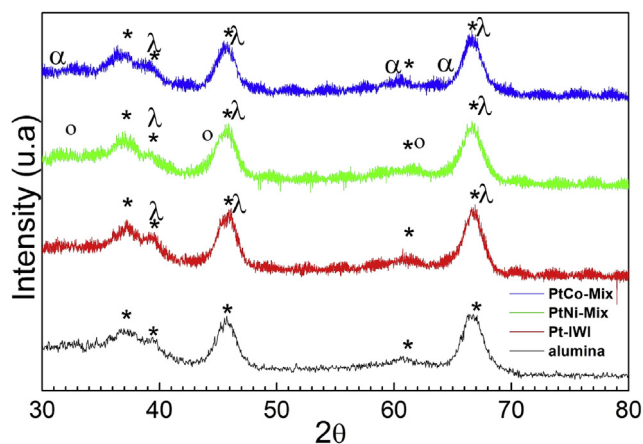


Fig. 7 – X-ray diffractograms of the studied catalysts.

Co doped catalysts. In the case of the Ni containing catalysts there are several oxidized species present and the spectra cannot be resolved due to the interfering effect of the signals of the alumina support.

The X-ray powder diffraction patterns of the prepared catalysts are shown in Fig. 7. We can see that all catalysts exhibited the peaks of gamma alumina at 2θ angles of 37, 39.2, 45.7, 61 and 67° [39]. Though the diffractograms showed practically no differences, in the case of Pt-IWI small differences in the peaks at 39.8°, 46.5° and 67.8° were detected [40]. The peak at 39.8° has been assigned to metallic (zero-valent) Pt [41]. PtNi-Mix showed NiO and/or NiAl₂O₄ peaks at 32.5°; 44°; 62° [9]. The PtCo-Mix catalyst had peaks attributed to Co₃O₄ and/or CoAl₂O₄ at 31°; 59.5° and 65° [9]. Low metal loads make it difficult to see bigger differences.

In Fig. 8 we can observe the TPR traces of the tested catalysts. The Pt-IWI catalyst had a peak at 503 K and another at 683 K, both corresponding to the reduction of Pt oxidized species [42]. The first peak was attributed to Pt species of easy access or low interaction with the support while the second

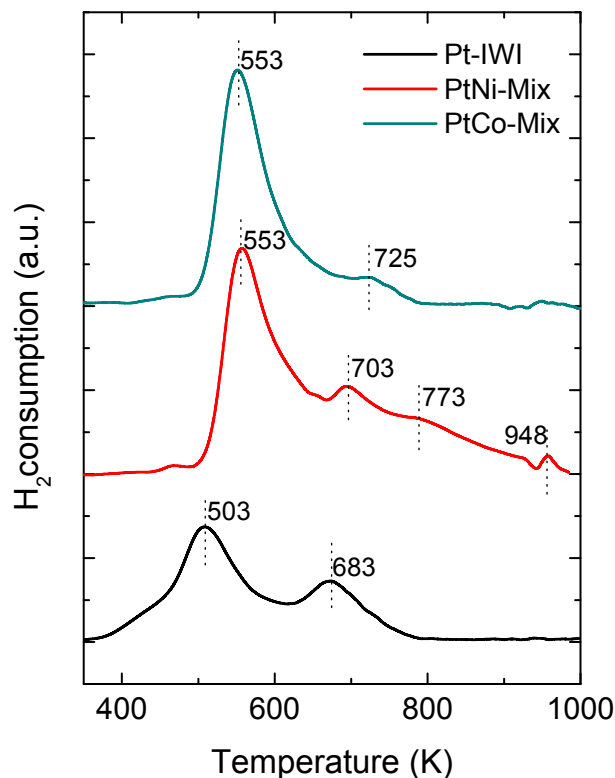


Fig. 8 – Temperature programmed reduction (TPR) traces of the studied catalysts.

would correspond to Pt species in strong interaction with the support, probably of the oxychlorided type. The lack of chlorine content could be responsible for a decrease in the reduction temperature [43].

In the case of the PtCo-Mix catalyst, the low temperature peak of Pt reduction is shifted to about 553 K due to the interference of Co ions. Hydrogen consumption in the region around 300–773 K has been attributed to the reduction of cobalt oxide, as Co₃O₄, along with the reduction of Co⁺³ surface ions [44]. The increase of the size of the first Pt reduction peak could thus be due to the co-reduction of Co and Pt species. The non-existence of a separate peak points to the close interaction between the two metal species of the metal function. The reduction of Co oxidized species at lower temperatures than those needed for pure bulk Co₃O₄ is attributed to the catalytic effect of Pt, which appears to promote the reduction of cobalt oxides through hydrogen spillover. Hydrogen dissociates on the surface of Pt and could migrate to the surface of Co₃O₄, resulting in Co being reduced at much lower temperatures in the bimetallic catalysts [45].

In the case of the PtNi-Mix catalyst a peak at 948 K can be seen. Other studies [46] have indicated that the reduction peak of NiO interacting with the support appears in the 773–973 K range. This is consistent with the XPS study. The peaks at 553 K and 703 K are mainly due to Pt reduction, the enlargement of the first peak being due to a co-reduction of Ni species in close interaction with Pt. The peak at 703 K would be due to Pt species in strong interaction with the support. The shoulder at 773 K is probably due to Ni species of intermediate reducibility.

Other authors have reported a broad reduction band extending from 300 to 700 K in Pt/Al₂O₃ catalysts with chlorine content (impregnated with H₂PtCl₆). In these cases, it is possible that the TPR profile include surface oxychloride species of the form Pt(OH)_xCl_y and PtO_xCl_y, in addition to PtO₂. This could produce a shift to higher temperatures in the low-temperature reduction peak of PtCo and PtNi, compared with the Pt-IWI catalyst, which not contain chlorine [47].

Table 1 also shows the consumption of H₂ during the temperature programmed reduction treatment. As shown, the bimetallic catalysts have a higher consumption than the Pt monometallic, indicating the co-reduction of Ni or Co atoms together with the Pt in both bimetallic.

Summarizing the characterization results for all catalysts it can be seen that Ni and Co addition both change the catalytic properties of the active sites. The effect seems to be related to a modification of the electronic density of Pt due to the Pt-Ni or Pt-Co interaction that explains the observed decrease in CO chemisorption capacity and activity for dehydrogenation.

EDAX results indicated that the surface Pt/promoter ratio is 1 Pt atom per 6 or 7 atoms of Ni or Co, a value close to the Pt:Ni, Pt:Co molar ratios used in the preparation of the catalysts. Some surface chlorine remains in the catalysts prepared from chloroplatinic acid. As measured by XPS, Pt²⁺ is the Pt most abundant species, and has the highest surface concentration. In the case of the Co doped catalyst, Co²⁺ is the dominant Co species. Several Ni oxidized species are detected in the Ni doped catalysts which could not be accurately identified due to the interfering effect of the alumina support.

The TPR traces of the bimetallic catalysts had larger Pt reduction peaks than those of the monometallic Pt-IWI catalysts. This was addressed to the co-reduction of Ni and Co species. Pt seemed to promote the reduction of cobalt oxides through hydrogen spillover. In agreement with the XPS results species of NiO interacting with the support were detected.

Catalytic activity results

APR of ethylene glycol

To take advantage of the greater number of metal anchoring sites generated by the CMU method and prevent Pt particles from being covered up by Ni or Co, bimetallic catalysts were prepared with a “mixed” technique with the addition of the Ni or Co promoter by the CMU method and the Pt precursor by the IWI method. Reforming of ethylene glycol was used to analyze the general catalytic performance of these catalysts in aqueous phase reforming (APR). Long term experiments were used to assess the catalyst stability since deactivation by coking or metal sintering could be possible. Results of hydrogen yield as a function of time-on-stream can be seen in Fig. 9. The pattern of increasing hydrogen yield is consistent with the reported by other authors [9]. It can be seen that the hydrogen yields got with the bimetallic catalysts are higher than that of the Pt-IWI catalyst. Catalysts PtCo-Mix and PtNi-Mix reach yield values almost 10% higher. One difference between these catalysts is that the activity of PtCo-Mix stabilizes at 400 min of reaction, while PtNi-Mix has a continuously increasing activity.

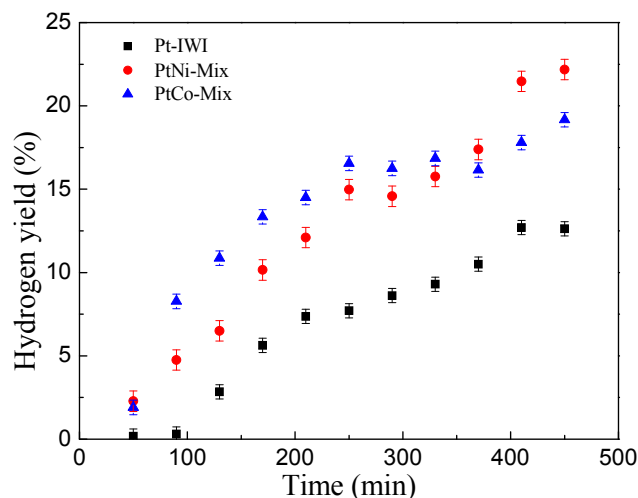


Fig. 9 – Hydrogen yield obtained in APR de Ethylene glycol (EG) with studied catalyst as a function of time-on-stream. Feed: aqueous solution of 10 %wt EG feed at 0.02 cm³min⁻¹. Operation conditions: 498 K, 2.2 MPa, 3 cm³min⁻¹ gas flow rate.

The catalytic selectivity was also influenced by the catalyst preparation procedure. Values of the carbon conversion from solution feed to gas product, selectivity to H₂, CH₄, CO and CO₂ and Turn-over-frequency for hydrogen production are indicated in Table 4. In the case of the bimetallic catalysts, the carbon conversion increases substantially with respect to monometallic catalyst in both cases, the selectivity to H₂ remained the same or even surpassed that of the control catalyst while the selectivity to CH₄ was similar to that of the Pt-IWI catalyst. The selectivity to CO shows that Ni does not favor the water gas shift (WGS) reaction, allowing the desorption of CO towards the gas phase. However the TOF^{H₂} value for PtNi catalyst is much superior to any other value of the tested group.

APR of glycerol and sorbitol

The reaction mechanism for the APR of glycerol and sorbitol leads to the same gas products as those proposed by Davda et al. [12] by APR of ethylene glycol. The scission of the C-C, C-H and C-O bonds demanded by this reaction mechanism occurs more easily on the surface of transition metal catalysts such as Pt, Pd, Rh and Ru [48]. Metals such as Pt or Pd show high activity for producing hydrogen while Ni is also active but produces more alkanes. The results of APR of ethylene glycol presented in this work indicate that Co also has an inhibiting effect on the formation of hydrocarbons (methane mainly) and can improve the overall activity and the selectivity to hydrogen.

The desired reaction pathway for the production of hydrogen from oxygenated compounds involves the scission of C-C bonds and C-H or O-H bonds to form CO adsorbed on the catalyst surface, followed by CO disposal by the water gas shift (WGS) exchange reaction to form CO₂ and H₂, since high amounts of CO on the catalyst surface lead to poor catalytic activity.

Table 4 – Values of Carbon conversion to gas (C Conv. to gas), selectivity to H₂, CH₄, CO and CO₂, obtained during the APR of ethylene glycol. Time-on-stream = 480 min. Turn-over-frequency for hydrogen production (TOF^{H₂}) in mol H₂ per min and per mol CO adsorbed on accessible metal site. Values of standard deviation (SD) for results are shown between parentheses.

Catalyst	C Conv. to gas, %	Selectivity				TOF ^{H₂} , min ⁻¹
		H ₂	CH ₄	CO	CO ₂	
Pt-IWI	43.5 (2.4)	36.3 (1.2)	0.8 (0.1)	1.7 (0.2)	97.5 (0.2)	0.9 (0.1)
PtNi-Mix	58.5 (1.1)	39.6 (0.7)	2.3 (0.1)	18.9 (0.7)	78.8 (0.7)	3.4 (0.1)
PtCo-Mix	49.3 (0.2)	37.1 (1.3)	1.9 (0.1)	0.9 (0.0)	97.2 (0.7)	1.7 (0.1)

Catalysts were tested in the same reaction system, under the same conditions of pressure and temperature, with a solution of 10% glycerol (mass basis). The time of reaction was 8 h and similar values of WHSV were used as in the case of ethylene glycol. The R factor for the glycerol reaction is 7/3.

The PtCo-Mix and PtNi-Mix catalysts had a high selectivity to H₂ and an excellent performance in this reaction. Fig. 10 shows a plot of the hydrogen yield values obtained with the standard Pt catalysts and the Mix catalysts. Both bimetallic catalysts show a pattern of increasing hydrogen yield throughout the experiment, differentiating them from Pt-IWI that had a declining yield pattern in the end of the test. This

would indicate that the Ni and Co promoters help maintaining the catalyst activity in a stable value. PtNi-Mix showed the highest hydrogen yield all throughout the test.

A comparison of all variables at the end of the run can be found in Table 5. Though the H₂ yield of the PtCo-Mix catalyst in these test was similar to that of the standard Pt catalyst, this catalyst had a higher selectivity to hydrogen. This could be related to its low methanation selectivity. In comparison the Ni doped catalyst had a very high hydrogen selectivity not only at the end of the run but during the whole run. It also had a high TOF^{H₂} in comparison to the other two catalysts. This is a feature already displayed in the EG tests.

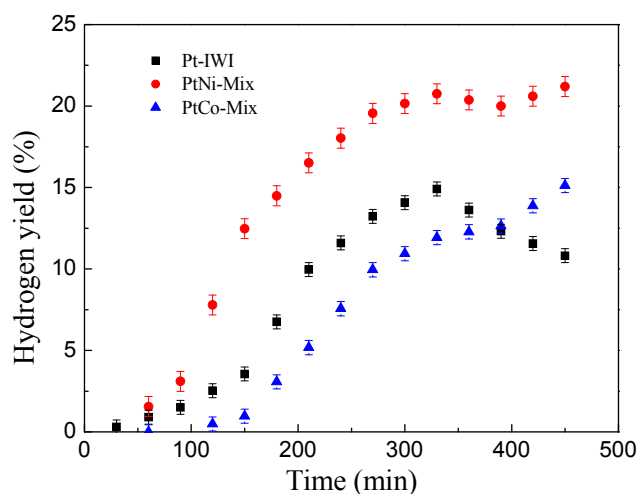


Fig. 10 – Hydrogen yield obtained in APR de Glycerol (Gly) with studied catalyst as a function of time-on-stream. Feed: aqueous solution of 10%wt Gly feed at 0.02 cm³min⁻¹. Operation conditions: 498 K, 2.2 MPa, 3 cm³min⁻¹ gas flow rate.

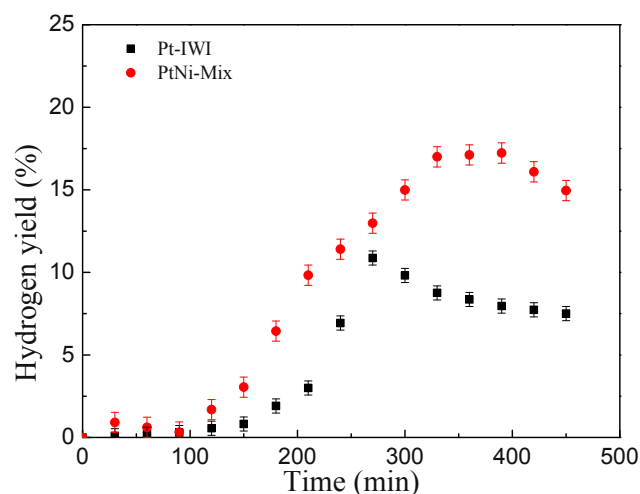


Fig. 11 – Hydrogen yield obtained in APR de Sorbitol (Sorb) with Pt-IWI and PtNi-Mix catalysts as a function of time-on-stream. Feed: aqueous solution of 10 %wt Sorb feed at 0.02 cm³min⁻¹. Operation conditions: 498 K, 2.2 MPa, 3 cm³min⁻¹ gas flow.

Table 5 – Values of Carbon conversion to gas (C Conv. to gas), selectivity to H₂, CH₄, CO and CO₂ during APR of glycerol. Time-on-stream = 480 min. Turn-over-frequency for hydrogen production (TOF^{H₂}) in mol H₂ per min and per mol CO adsorbed on accessible metal site. Values of standard deviation (SD) for results are shown between parentheses.

Catalyst	C Conv. to gas, %	Selectivity				TOF ^{H₂} , min ⁻¹
		H ₂	CH ₄	CO	CO ₂	
Pt-IWI	31.1 (0.6)	35.6 (0.7)	15.0 (0.4)	0.7 (0.2)	85.0 (0.7)	0.7 (0.0)
PtNi-Mix	43.3 (0.7)	41.7 (0.4)	11.0 (0.2)	0.0 (0.0)	86.6 (0.2)	2.6 (0.4)
PtCo-Mix	22.7 (0.5)	55.5 (1.6)	7.7 (0.0)	0.0 (0.0)	92.3 (0.0)	1.2 (0.2)

Table 6 – Values of Carbon conversion to gas (C Conv. to gas), selectivity to H₂, CH₄, CO and CO₂ during APR of sorbitol. Time-on-stream = 480 min. Turn-over-frequency for hydrogen production (TOF^{H₂}) in mol H₂ per min and per mol CO adsorbed on accessible metal site. Values of standard deviation (SD) for results are shown between parentheses.

Catalyst	C Conv.to gas. %	Selectivity				TOF ^{H₂} , min ⁻¹
		H ₂	CH ₄	CO	CO ₂	
Pt-IWI	21.7 (0.8)	34.5 (0.0)	8.8 (0.1)	0.7 (0.0)	90.5 (0.1)	0.4 (0.0)
PtNi-Mix	42.1 (1.6)	35.5 (0.2)	9.4 (0.6)	0.0 (0.0)	90.6 (0.6)	0.9 (0.1)

Table 7 – Values of coke content on the used catalysts after the APR of ethylene glycol, glycerol and sorbitol at long reaction times (TOS = 600 min).

Catalizador	% C		
	Ethylene glycol	Glycerol	Sorbitol
Pt-IWI	1.4	1.6	7.5
PtNi-Mix	6.5	8.2	11.4
PtCo-Mix	1.8	2.5	–

In other reports Nichio et al. [49] got H₂ yields that result very low compared to those of this work, although the Pt content of their catalysts was different (2%). Kim et al. [50,51] obtained similar or higher H₂ yields, even higher H₂ selectivity in APR of glycerol, but in those cases, the Pt content of the catalysts was about 7%. Comparing with other works, a better catalytic performance of PtNi and PtCo catalysts over Pt-IWI catalysts can be seen.

After these experiments, catalysts were tested in the same reaction system, under the same conditions of pressure and temperature, with a solution of 10% sorbitol. Reaction time was 8 h, spatial velocity values were similar to those of the previous test. The R factor for this reaction was 13/6.

As it can be seen in Fig. 11 the hydrogen yield of the PtNi-Mix catalyst is higher than that of the Pt-IWI catalyst at all values of time-on-stream. When the stability is considered, for both catalysts a slight decline in hydrogen yield at the end of the run was detected. In the APR of glycerol an improvement in the stability of the PtNi-Mix catalyst had been found with respect to the other catalysts. In this case a stability improvement can be seen, since the activity decline is only detected in the last hour of the test.

The standard Pt-IWI catalyst exhibited increasing hydrogen yields until 300 min time-on-stream, declining afterwards. The big difference in hydrogen yield with the other catalyst is related to this final loss of reforming activity.

These results may be related to the presence of a greater concentration of metals with reforming capacity (Pt and Ni) in the case of the PtNi catalyst. The reforming activity could be favored by the co-reduction of Ni species in close interaction with Pt.

It is possible to observe in Table 6 that H₂ selectivity reached similar levels in both catalysts and this are close to the selectivity of Pt-IWI in APR of glycerol. Other authors found analogous values of H₂ selectivity for APR of an aqueous solution of 1% of sorbitol [52]. TOF^{H₂} values are similar in this case; however, PtNi-Mix shows a high value of turnover frequency.

Coke deposition

Table 7 shows the results of temperature programmed oxidation of the carbon deposits accumulated on the catalysts during the reactions of APR of polyols. The Pt-IWI catalyst had the lowest coke concentration.

As many more molecules were reformed on the PtNi higher coke contents should be formed on it. However there seems to be too much a difference in coke content between the Pt and the PtNi catalysts to be solely explained by the different reforming activity levels found in the tests. Probably the Pt monometallic function had a higher activity for hydrogenolysis of coke precursors adsorbed on it. It is reasonable to assume that the coke content over a catalyst with low amount of metal is the cause of its deactivation. PtNi and PtCo catalysts had a higher metal content and they could maintain their reforming activity for longer periods of time.

Conclusions

It was possible to prepare PtNi and PtCo catalysts supported on alumina with good H₂ production by APR of polyols by combining two techniques: urea matrix combustion for dispersing Ni and Co, and incipient wetness impregnation for incorporating Pt. We called this combination CMU-IWI, or “mixed” technique. CMU-IWI allowed achieving high final Ni and Co dispersion values and good degrees of metal-metal interaction as shown by SEM, XPS and TPR results. This technique permitted reducing the total charge of the promoter metal, increasing the performance of the metallic function and increasing the stability under reaction conditions. The little changes in the acidity of the support generated by impregnation with H₂Cl₆Pt did not modify the selectivity while the increase of the Pt dispersion improved the activity and stability of the catalyst in the APR of polyols.

SEM-EDAX, XRD and N₂ adsorption analysis showed that the preparation methods did not modify the support surface. They also detected a high concentration of promoter (Ni or Co) on the surface interacting with the Pt atoms.

In APR of ethylene glycol, platinum showed high yields and selectivity to hydrogen. Cobalt addition to Pt, improved the carbon conversion to gas product, the activity in WGS, the yield and the TOF^{H₂}. Methanation was also inhibited. Nickel was the best promoter of Pt because of its good activity for reforming, but its low activity in WGS increase the relative importance on the methanation reaction, thus decreasing the net capacity for generating hydrogen. In any case, the catalytic activity was improved more than 50%, with a high yield, selectivity and TOF for hydrogen production.

According to the pattern of hydrogen yield of the experiments, Ni and Co promoters helped maintaining the catalyst activity. Ni displayed higher H₂ yield values in glycerol and sorbitol reforming too, and showed excellent selectivity to hydrogen and a good stability. PtNi-Mix maintained a capacity for generating hydrogen unaffected for long periods of time. This quality was attributed to the presence of Ni and Pt, metals very active in the reforming reactions. Co addition helped in keeping low levels of coke and a low selectivity to methane. This catalyst also had the highest value of TOF^{H₂} in all the experiments, even when glycerol was the feedstock.

Acknowledgements

The authors thank the financial support of CONICET (PIP Grant 2014-560), Universidad Nacional del Litoral (CAI+D Grant 2011-155) and ANPCyT (PICT Grant 2013- 3217). They also thank SASOL for donation of alumina used in this paper.

REFERENCES

- [1] Wuebbles DJ, Jain AK. Concerns about climate change and the role of fossil fuel use. *Fuel Process Technol* 2001;71:99–119.
- [2] Chmielewski AG. Environmental effects of fossil fuel combustion. In: Goldemberg J, editor. *Interactions: energy/ environment. Encyclopedia of life support systems (EOLSS)*; 2011. p. 56–74.
- [3] Tanksale A, Beltramini JN, Lu GM. A review of catalytic hydrogen production processes from biomass. *Renew Sustain Energy Rev* 2010;14:166–82.
- [4] Rinaldi R, Schüth F. Acid hydrolysis of cellulose as the entry point into biorefinery schemes. *ChemSusChem* 2009;2:1096–107.
- [5] Al-Zuhair S, Ahmed K, Abdulrazak A, El-Naas MH. Synergistic effect of pretreatment and hydrolysis enzymes on the production of fermentable sugars from date palm lignocellulosic waste. *J Ind Eng Chem* 2013;19:413–5.
- [6] Huber GW, Dumesic JA. An overview of aqueous-phase catalytic processes for production of hydrogen and alkanes in a biorefinery. *Catal Today* 2006;111:119–32.
- [7] Balat H, Kirtay E. Hydrogen from biomass - present scenario and future prospects. *Int J Hydrog Energy* 2010;35:7416–26.
- [8] Cheng Ch K, Foo SY, Adesina AA. H₂-rich synthesis gas production over Co/Al₂O₃ catalyst via glycerol steam reforming. *Catal Commun* 2010;12:292–8.
- [9] Luo N, Fu X, Cao F, Xiao T, Edwards PP. Glycerol aqueous phase reforming for hydrogen generation over Pt catalyst – effect of catalyst composition and reaction conditions. *Fuel* 2008;87:3483–9.
- [10] Cortright RD, Davda RR, Dumesic JA. Hydrogen from catalytic reforming of biomass-derived hydrocarbons in liquid water. *Nature* 2002;418:964–7.
- [11] Cao C, Wang Y, Rozmiarek R. Heterogeneous reactor model for steam reforming of methane in a microchannel reactor with microstructured catalysts. *Catal Today* 2005;110:92–7.
- [12] Davda RR, Shabaker JW, Huber RD, Cortright RD, Dumesic JA. A review of catalytic issues and process conditions for renewable hydrogen and alkanes by aqueous-phase reforming of oxygenated hydrocarbons over supported metal catalysts. *Appl Catal B Environ* 2005;56:171–86.
- [13] Huber GW, Shabaker JW, Evans ST, Dumesic JA. Aqueous-phase reforming of ethylene glycol over supported Pt and Pd bimetallic catalysts. *Appl Catal B Environ* 2006;62:226–35.
- [14] Kim H, Kim T, Park HJ, Jeong K, Chae H, Jeong S, et al. Hydrogen production via the aqueous phase reforming of ethylene glycol over platinum-supported ordered mesoporous carbon catalysts: effect of structure and framework-configuration. *Int J Hydrog Energy* 2012;37:12187–97.
- [15] Kim M, Kim T, Kim H, Kim C, Bae J. Aqueous phase reforming of polyols for hydrogen production using supported Pt-Fe bimetallic catalysts. *Renew Energy* 2016;95:396–403.
- [16] van Haasterecht T, Ludding CCI, de Jong KP, Bitter JH. Stability and activity of carbon nanofiber-supported catalysts in the aqueous phase reforming of ethylene glycol. *J Energy Chem* 2013;22:257–69.
- [17] Jeong S, Park YM, Saravanan K, Han GY, Kim B, Lee J, et al. Aqueous phase reforming of ethylene glycol over bimetallic platinum-cobalt on ceria-zirconia mixed oxide. *Int J Hydrog Energy* 2017;42:9892–902.
- [18] Rahman MM. H₂ production from aqueous-phase reforming of glycerol over Cu-Ni bimetallic catalysts supported on carbon nanotubes. *Int J Hydrog Energy* 2015;40:14833–44.
- [19] Duarte HA, Sad ME, Apesteguía CR. Aqueous phase reforming of sorbitol on Pt/Al₂O₃: Effect of metal loading and reaction conditions on H₂ productivity. *Int J Hydrog Energy* 2016;41:17290–6.
- [20] González-Cortés S, Xiao T, Green M. *Scientific bases for the preparation of heterogeneous catalysts*. first ed. Oxford: Elsevier; 2006. p. 817–24.
- [21] González-Cortés SL, Imbert FE. Fundamentals, properties and applications of solid catalysts prepared by solution combustion synthesis (SCS). *Appl Catal A Gen* 2013;452:117–31.
- [22] Varma A, Mukasyan AS, Rogachev AS, Manukyan KV. Solution combustion synthesis of nanoscale materials. *Chem Rev* 2016;116(23):14493–586.
- [23] Bournonville JP, Martino G. Sintering of alumina supported platinum. *S.S Sci Catal* 1980;6:159–66.
- [24] Boudart M, Aldag A, Benson JE, Dougharty NA, Harkins CG. On the specific activity of platinum catalysts. *J Catal* 1996;6:92–9.
- [25] Davda RR, Shabaker JW, Huber GW, Cortright RD, Dumesic JA. Aqueous-phase reforming of ethylene glycol on silica-supported metal catalysts. *Appl Catal B Environ* 2003;43:13–26.
- [26] Shabaker JW, Davda RR, Huber GW, Cortright RD, Dumesic JA. Aqueous-phase reforming of methanol and ethylene glycol over alumina-supported platinum catalysts. *J Catal* 2003;215:344–52.
- [27] Shabaker JW, Huber GW, Dumesic JA. Aqueous-phase reforming of oxygenated hydrocarbons over Sn-modified Ni catalysts. *J Catal* 2004;222:180–91.
- [28] Ko E, Park E, Seo KW, Lee HC, Lee D, Kim S. Pt–Ni/γ-Al₂O₃ catalyst for the preferential CO oxidation in the hydrogen stream. *Catal Lett* 2006;110:275–9.
- [29] Fogar K. In: *Catalysis science and technology, chapter 4 dispersed metal catalysts*, vol. 6. New York, NY: Springer-Verlag; 1984. p. 227–305.
- [30] Escaño MC, Gyenge E, Nakanishi H, Kasai H. Pt/Cr and Pt/Ni catalysts for oxygen reduction reaction: to alloy or not to alloy? *J Nanosci Nanotechnol* 2011;11:2944–51.
- [31] Corro G, Fierro JLG, Odilon VC. An XPS evidence of Pt_{4p} present on sulfated Pt/Al₂O₃ and its effect on propane combustion. *Catal Commun* 2003;4:371–6.
- [32] Serrano-Ruiz JC, Huber GW, Sánchez-Castillo MA, Dumesic JA, Rodríguez-Reinoso F, Sepúlveda-Escribano A. Effect of Sn addition to Pt/CeO₂–Al₂O₃ and Pt/Al₂O₃ catalysts:

- an XPS, ^{119}Sn Mössbauer and microcalorimetry study. *J Catal* 2006;241:378–88.
- [33] Shyu JZ, Otto K. Identification of platinum phases on γ -alumina by XPS. *Appl Surf Sci* 1998;32:246–52.
- [34] Ciuparu D, Pfefferle L. Support and water effects on palladium based methane combustion catalysts. *Appl Catal A Gen* 2001;209:415–28.
- [35] Rodriguez NM, Oh SG, Dalla Betta RA, Baker RTK. In-situ electron microscopy studies of palladium supported on Al_2O_3 - SiO_2 , and ZrO_2 in oxygen. *J Catal* 1995;157:676–86.
- [36] Otto K, Haack LP, de Vries JE. Identification of two types of oxidized palladium on γ -alumina by X-ray photoelectron spectroscopy. *Appl Catal B Environ* 1992;1:1–12.
- [37] Jiang Y, Kang Q, Zhang J, Dai H, Wang P. Novel sulfonated poly (ether ether ketone)/phosphonic acid-functionalized titanianano hybrid membrane by an in situ method for direct methanol fuel cells. *J Power Sources* 2015;273:554–60.
- [38] Shalvoy RB, Davis BH. Studies of the metal–support interaction in coprecipitated nickel on alumina methanation catalysts using X-ray photoelectron spectroscopy (XPS). *Surf Interface Anal* 1980;2:11–6.
- [39] Joint Committee on Powder Diffraction Standards (JCPDS) card N°; 86–1410.
- [40] El Doukkali M, Iriondo A, Arias PL, Requies J, Gandarías I, Jalowiecki-Duhamel L, et al. A comparison of sol–gel and impregnated Pt or/and Ni based -alumina catalysts for bioglycerol aqueous phase reforming. *Appl Catal B Environ* 2012;125:516–29.
- [41] Persson K, Ersson A, Colussi S, Trovarelli A, Järås SG. Catalytic combustion of methane over bimetallic Pd–Pt catalysts: the influence of support materials. *Appl Catal B Environ* 2006;66:175–85.
- [42] Jia J, Shen J, Lin L, Xu Z, Zhang T, Liang D. A study on reduction behaviors of the supported platinum–iron catalysts. *J Mol Catal A Chem* 1999;138:177–84.
- [43] Liu X, Yang Y, Zhang J. Temperature-programmed reduction and desorption studies of praseodymium promoted platinum/alumina catalysts. *Appl Catal* 1991;71:167–84.
- [44] Liotta LF, Pantaleo G, Macaluso A, Di Carlo G, Deganello G. CoOx catalysts supported on alumina and alumina-baria: influence of the support on the cobalt species and their activity in NO reduction by C_3H_6 in lean conditions. *Appl Catal A Gen* 2003;245:167–77.
- [45] Lu S, Lonergan WW, Bosco JP, Wang S, Zhu Y, Xie Y, et al. Low temperature hydrogenation of benzene and cyclohexene: a comparative study between γ - Al_2O_3 supported PtCo and PtNi bimetallic catalysts. *J Catal* 2008;259:260–8.
- [46] Shang Z, Li S, Li L, Liu G, Liang X. Highly active and stable alumina supported nickel nanoparticle catalysts for dry reforming of methane. *Appl Catal B Environ* 2017;201:302–9.
- [47] Navarro RM, Pawelec B, Trejo JM, Mariscal R, Fierro JLG. Hydrogenation of aromatics on sulfur-resistant PtPd bimetallic catalysts. *J Catal* 2000;189:184–94.
- [48] Huber GW, Dumesic JA. An overview of aqueous-phase catalytic processes for production of hydrogen and alkanes in a biorefinery. *Catal Today* 2006;111:119–32.
- [49] Barbelli ML, Pompeo F, Santori GF, Nichio NN. Pt catalyst supported on - Al_2O_3 modified with CeO_2 and ZrO_2 for aqueous-phase-reforming of glycerol. *Catal Today* 2013;213:58–64.
- [50] Kim T, Park HJ, Yang Y, Jeong S, Kim C. Hydrogen production via the aqueous phase reforming of polyols over three dimensionally mesoporous carbon supported catalysts. *Int J Hydrog Energy* 2014;39:11509–16.
- [51] Jeong K, Kim H, Kim T, Kim J, Chae H, Jeong S, et al. Hydrogen production by aqueous phase reforming of polyols over nano- and micro-sized mesoporous carbon supported platinum catalysts. *Catal Today* 2014;232:151–7.
- [52] Neira D'Angelo MF, Ordonsky V, van der Schaaf J, Schouten JC, Nijhuis TA. Continuous hydrogen stripping during aqueous phase reforming of sorbitol in a wash coated micro-channel reactor with a Pt-Ru bimetallic catalyst. *Int J Hydrog Energy* 2014;39:18069–76.